Digital Sliding Mode Control of Anti-Lock Braking System

Darko B. MITIĆ, Staniša Lj. PERIĆ, Dragan S. ANTIĆ,
Zoran D. JOVANOVIĆ, Marko T. MILOJKOVIĆ, Saša S. NIKOLIĆ
University of Niš, Faculty of Electronic Engineering, Department of Control Systems
Aleksandra Medvedeva 14, 18000 Niš, Serbia, Phone: (+381) 18 529-363
stanisa.peric@elfak.ni.ac.rs

***Abstract*—The control of anti-lock braking system is a great challenge, because of the nonlinear and complex characteristics of braking dynamics, unknown parameters of vehicle environment and system parameter variations. Using some of robust control methods, such as sliding mode control, can be a right solution for these problems. In this paper, we introduce a novel approach to design of ABS controllers, which is based on digital sliding mode control with only input/output measurements. The relay term of the proposed digital sliding mode control is filtered through digital integrator, reducing the chattering phenomenon in that way, and the additional signal of estimated modelling error is introduced into control algorithm to enhance the system steady-state accuracy. The given solution was verified in real experimental framework and the obtained results were compared with the results of implementation of two other digital sliding mode control algorithms. It is shown that it gives better system response, higher steady-state accuracy and smaller chattering.**

***Index Terms*—anti-lock braking system, discrete-time nonlinear model, modelling error estimation, quasi-sliding mode, wheel slip control.**

I. INTRODUCTION

Anti-lock braking system (ABS) is an electronic system, whose main goal is to prevent locking of wheels due to suddenly braking, ensuring the best wheel to road surface adhesion, and to provide better steering of vehicle in that way. These systems have been used since 1964, and they are standard equipment in the most of modern vehicles.

The adhesion between wheel and road surface is usually specified by a coefficient of road adhesion μ, representing the coefficient of proportion between the friction force and the normal load of the vehicle. It depends on a wheel slip λ - a relative difference between the speeds of the wheel and the vehicle. The wheel slip should be set to the constant value by a controller, so that the coefficient of road adhesion has a maximum value. According to [1], the optimal values of wheel slip are between 0.08 and 0.3. Another approach is to estimate the value of wheel slip in real time, for which the road friction curve has its maximum [2].

ABS mathematical model is strongly nonlinear because of nonlinear characteristics of braking dynamics with unknown parameters of vehicle environment. Furthermore, due to components deterioration, the known system parameters also vary, and many external disturbances, acting on ABS, cannot be predicted in advance. The survey of control approaches used in design of ABS is given in [3].

The design of linear PI, gain-scheduling, and fuzzy control based on linearized ABS models is discussed in [4], by using the results obtained in the similar experimental framework as in this paper. A genetic fuzzy self-tuning PID control of ABS is developed in [5]. An interpolative and Takagi-Sugeno fuzzy controllers are presented in [6] for slip control. Two original model-based fuzzy control solutions, dedicated to the slip control of ABS laboratory equipment, are given in [7].

In order to cope with ABS non-linearity and parameter uncertainties, robust non-linear control algorithms should be used. The integration of the non-linear ABS control and the active suspension system would provide further enhancement of the system performance [8]. Sliding mode control (SMC) algorithms [9-10] could be the good choice in ABS control applications, as well.

SMC belongs to one class of nonlinear discontinuous control algorithms. Sliding mode (SM) exists when the control ensures system state motion along predefined sliding hyper-surface, defined by switching function. When in SM, a system is robust to parameter variations and external disturbances. This is of great importance in control of nonlinear systems such as ABS. The high-frequency nature of SMC signal is the main drawback of this control method, because the control can excite non-modelled system dynamics and wear out ABS mechanical parts. This phenomenon is known as a chattering. Fuzzy control techniques, usually implemented to suppress the chattering problem, can be used to cope with modelling uncertainties of nonlinear system, parameter perturbations and external disturbances, as well [11-12].

There are many papers dealing with the implementation of SMC in ABS. In [13], SMC is enhanced by a grey system theory and implemented in ABS control. The engine torque is used to control wheel slip in [14], where the existence of sliding motion is ensured by moving sliding surface. To cope with chattering phenomenon, the integral switching function is treated in [15]. The traditional SMC of magneto rheological brake system is presented in [16]. In [17], the hydraulic brake dynamics is included in design of ABS with conventional SMC. The combination of SMC and sliding mode observer is elaborated in [18]. The adaptive SMC method is discussed in [19], where only the difference between vehicle and wheel speeds is used instead of the wheel slip. The SMC with the neural networks and the moving sliding surface is considered in [20]. The combination of SMC and pulse width modulation (PWM)

This paper was realized as a part of the projects TR 35005 and III 44006, financed by the Ministry of Education and Science of the Republic of Serbia for the period 2011-2014.

Digital Object Identifier 10.4316/AECE.2013.01006

method, is treated in [21-22]. In [23], the novel nonlinear control with integral feedback is compared with SMC. In order to provide overall vehicle stability, SMC is implemented for wheel slip control, and the linear quadratic regulator is used as a yaw moment controller [24]. The combination of SMC and fuzzy control (FC) is elaborated in [25]. The fuzzy blocks of FC are utilized to calculate the parameters of the constant plus proportional rate reaching law of SMC [26]. A comparative analysis of several continuous-time SMCs of ABS is presented in [27], both with a brief overview of existing SMC concepts in continuous-time domain. In this paper, we propose the novel approach in design of ABS control based on the digital SMC.

SMC implementation on microcontrollers requires the discretization process of SMC, resulting in the quasi-sliding motion [28] and producing chattering in the $O(T)$ vicinity of a sliding hyper-surface, where T is a sampling period. The overview of digital SMC systems is presented in [29]. The control approach for ABS, proposed in this paper, belongs to the group of input/output based digital SMC algorithms. There are two possible solutions to digital SM controller design of nonlinear plant. The first one is based on discrete-time representation of linearized plant model [30] and the use of (generalized) minimum variance control in combination with digital SMC [31-33]. This method should be superior in comparison to the traditional linear control techniques. The second solution uses the input/output discrete-time nonlinear plant models in digital SMC design [34]. Such an approach is implemented in control of ABS in [35]. The control algorithm for ABS, proposed and implemented in this paper, combines the solution presented in [33] for linear plants with the control law given in [34]. The result is the robust control law that could suppress the chattering phenomenon, thanks to filtering of the sliding mode relay control component [35-37], and, at the same time, provide high system steady-state accuracy by introducing estimated modelling error signal into the control.

The paper is organized as follows. In Section II, the basics of proposed digital SMC algorithm, implemented in ABS, are presented. Section III describes ABS experimental framework. The continuous- and discrete-time models of ABS are given in Section IV. In Section V, the novel digital SMC algorithm is adjusted and applied on ABS. The experimental results are presented and discussed in Section VI. Concluding remarks are given in Section VII.

II. Digital SMC Based on Nonlinear Plant Model

Let us consider a single-input-single-output nonlinear plant in the following form:

$$y_{k+1} = f\left(y_k,\ldots,y_{k-n}\right) + g\left(y_k,\ldots,y_{k-n}\right)u_k, \qquad (1)$$

where y_k represents a plant output, u_k is a control output, n is a positive integer number determining plant order, whereas $f\left(y_k,\ldots,y_{k-n}\right)$ and $g\left(y_k,\ldots,y_{k-n}\right)$ represent smooth nonlinear functions of plant output and its past values. Notice that the plant model is linear in relation to the control input u_k.

In further text we will use the abbreviations $f_k = f\left(y_k,\ldots,y_{k-n}\right)$ and $g_k = g\left(y_k,\ldots,y_{k-n}\right)$, where g_k is a strictly positive and limited function away from zero. Due to uncertainties and variations of plant parameters, the nominal plant model:

$$y_{k+1} = \hat{f}\left(y_k,\ldots,y_{k-n}\right) + \hat{g}\left(y_k,\ldots,y_{k-n}\right)u_k, \qquad (2)$$

is used in design process, where $\hat{f}_k = \hat{f}\left(y_k,\ldots,y_{k-n}\right)$ and $\hat{g}_k = \hat{g}\left(y_k,\ldots,y_{k-n}\right)$ denote nominal functions of f_k and g_k, respectively, whereas $\hat{g}_k$ retains the assumed characteristics of g_k, previously mentioned. In that case, there is a modelling error determined by:

$$\varepsilon_{k+1} = y_{k+1} - \hat{y}_{k+1} = f_k - \hat{f}_k + \left(g_k - \hat{g}_k\right)u_k, \qquad (3)$$

which is upper bounded:

$$\max\left|\varepsilon_k\right| < E, \ \forall k. \qquad (4)$$

Suppose that reference input signal is *a priori* known as an output of reference system defined as:

$$r_{k+1} = a_0 r_k + \ldots + a_n r_{k-n} + b_0\rho_k + \ldots + b_m\rho_{k-m}, \qquad (5)$$

where $a_0,\ldots,a_n$ and $b_0,\ldots,b_m$ represent coefficients of stable polynomials $A\left(z^{-1}\right) = a_0 + a_1 z^{-1} + \ldots + a_n z^{-n}$ and $B\left(z^{-1}\right) = b_0 + b_1 z^{-1} + \ldots + b_m z^{-m}$, respectively, z is a complex variable, z^{-1} denotes a unit delay (delay operator), and ρ_k is an input of reference system. Tracking error is now defined as:

$$e_k = y_k - r_k. \qquad (6)$$

Taking into account (3), the plant model (1) can be rewritten as:

$$y_{k+1} = \varepsilon_{k+1} + \hat{f}_k + \hat{g}_k u_k. \qquad (7)$$

The main goal of control design is to find a digital SMC, which can provide a zero value of switching function:

$$s_k = c_0 e_k + c_1 e_{k-1} + \ldots + c_n e_{k-n}, \qquad (8)$$

where $c_0,\ldots,c_n$ are coefficients of the polynomial $C\left(z^{-1}\right) = c_0 + c_1 z^{-1} + \ldots + c_n z^{-n}$, with roots inside the unit disk in the z-plane. Notice that the tracking error e_k will converge to zero asymptotically if quasi-sliding mode exists in a system, i.e., $s_k = 0$.

In order to achieve the control design objective, we propose a digital SMC algorithm in the following form:

$$u_k = -\frac{1}{c_0\hat{g}_k}\left(\begin{array}{l} c_0\left(\hat{f}_k - r_{k+1}\right) + c_1 e_k + \ldots + \\ + c_n e_{k-n+1} + \dfrac{\alpha T}{1-z^{-1}}\operatorname{sgn}\left(s_k\right) + c_0\varepsilon_k \end{array}\right), \qquad (9)$$

where α is a positive real constant parameter, T is a sampling period (as a part of discrete-time integrator $T/(1-z^{-1})$), and ε_k is an output of one-step delayed modelling error estimator defined as:

$$\varepsilon_k = y_k - \hat{f}_{k-1} - \hat{g}_{k-1}u_{k-1}. \qquad (10)$$

Notice that the chattering is significantly reduced since the high-frequency relay component of the control signal is passed through the digital integrator acting as a low-pass filter. Substituting (9) in (7) yields the equation of switching function dynamics as:

$$s_{k+1} = s_k - \alpha T\operatorname{sgn}\left(s_k\right) + c_0\left(\varepsilon_{k+1} - 2\varepsilon_k + \varepsilon_{k-1}\right). \qquad (11)$$

To provide stable switching function dynamics, the value of parameter α should be chosen according to the following Theorem 1.

Theorem 1: *If the parameter α is chosen to satisfy the following inequality:*

$$\alpha T > \Delta E > \max\left|c_0\left(\varepsilon_{k+1} - 2\varepsilon_k + \varepsilon_{k-1}\right)\right|, \quad (12)$$

where ΔE is positive real number, then, for every initial state s_0, there exists an integer number $K_0 = K_0(s_0)$, such that for every $k \geq K_0$, system phase trajectory, described by (11) and (12), enters the domain $S(T)$ defined by:

$$S(T) = \left\{s_k : |s_k| < \alpha T + \Delta \mathrm{E}\right\}, \quad (13)$$

and remains in it for every $k = K_0 + m$, where m is a random positive integer number.

Proof: See Appendix A.

The overall system stability is ensured if and only if the conditions of the next Theorem are fulfilled.

Theorem 2: *System described by (7), (8) and (9) is stable if and only if:*

1) *inequality (12) is satisfied for every k, i.e., quasi-sliding mode exists in the system, and*
2) *polynomial $C\left(z^{-1}\right)$ has its roots inside the unit disk in z-plane.*

Proof: If the parameter α is chosen to satisfy inequality (12), then, according to Theorem 1, the quasi-sliding mode exists in the domain $S(T)$. Now, we can see from (8) that y_k will converge to the reference input signal r_k if and only if the polynomial $C\left(z^{-1}\right)$ is stable.

System steady-state accuracy directly depends on the difference $c_0\left(\varepsilon_{k+1} - 2\varepsilon_k + \varepsilon_{k-1}\right)$, as $e_\infty = s_\infty / C(1)$ according to (8), and αT is chosen to be slightly greater than ΔE, i.e., $\max\left|c_0\left(\varepsilon_{k+1} - 2\varepsilon_k + \varepsilon_{k-1}\right)\right|$. Since a non-linear plant model is originally continuous-time before discretization, the outputs of plant y and its nominal model $\hat{y}$ as well as the modelling error $\varepsilon = y - \hat{y}$ are also considered continuous. Suppose that ε is twice differentiable on the interval $(kT - T, kT + T)$. Then, it is possible to show that $c_0\left(\varepsilon_{k+1} - 2\varepsilon_k + \varepsilon_{k-1}\right)$ has $O\left(T^2\right)$ accuracy by using the Lagrange's theorem in the following manner:

$$\begin{aligned} &\varepsilon_{k+1} - 2\varepsilon_k + \varepsilon_{k-1} = \\ &= T\dot{\varepsilon}(t)\Big|_{t=kT+\zeta_k} - T\dot{\varepsilon}(t)\Big|_{t=kT-T+\zeta_{k-1}} = \\ &= T\left(T + \zeta_k - \zeta_{k-1}\right)\ddot{\varepsilon}(t)\Big|_{t=kT+\zeta_{k-1,k}}, \end{aligned} \quad (14)$$

where $\zeta_{k-1}, \zeta_k \in (0,T)$, $\zeta_{k-1,k} \in (0,T)$ and $|\zeta_k - \zeta_{k-1}| < T$. Accordingly, if $|\ddot{\varepsilon}(t)| < \mathrm{E}'' = \text{const.}$, then:

$$\varepsilon_{k+1} - 2\varepsilon_k + \varepsilon_{k-1} < \mathrm{E}''T^2 = O\left(T^2\right), \quad (15)$$

and the accuracies of s_k and e_k are determined by $O\left(T^2\right)$ and $O\left(T^2\right)/C(1)$, respectively. It is obvious that they are smaller than the accuracies obtained by the control algorithm given in [34-37].

III. ABS Framework

Practical ABS framework, used in experiments performed in this paper, is made by Inteco, Poland [38]. It contains two wheels, where the upper one represents a wheel of the vehicle, while the lower one animates relative road motion and it can be covered with some material to simulate road surface (ice, snow, rain etc.). The braking mechanism, mounted on the upper wheel, is connected to the brake lever via hydraulic coupling. A small DC motor drives the brake lever via steel cord and tightening pulley. This steel cord introduces an additional nonlinearity in system and limits the control input signal on 50% of its maximum nominal value. A large DC motor drives and accelerates the lower wheel in the acceleration phase, while its power supply is turned off in the braking phase.

The encoders, used as angular position sensors, measure angles with 0.175° precision and they are installed on both wheels. The wheel angular velocities are estimated by using the Euler formula with 0.5 ms sampling time period. The described mechanism is connected to PC via hardware interface corresponding to control unit of standard ABS. The purpose of this interface is to amplify control signals and to convert the encoders pulse signals to the digital 16-bit number. The whole logic is configured in the Xilinx® chip of the RT-DAC4/USB board and all board functions can be accessed from the ABS Toolbox, operating in MATLAB®/Simulink® and RTWT toolbox environment.

IV. ABS Mathematical Models

Graphical representation of ABS for quarter vehicle is presented in Fig. 1. The given ABS model considers only the longitudinal motion of vehicle and the rotation of wheel. The interaction of wheels is not taken into account, as well. This simplified model does not represent full complexity of the real system but it determines system dynamics adequately enough.

As it can be seen from Fig. 1, the vehicle (wheel) velocity is equal to the angular velocity of the lower (upper) wheel multiplied by its radius. Three torques act on the upper wheel: the friction torque in the upper bearing, the friction torque among the wheels, and the brake torque M_1.

On the other side, there are two friction torques acting on the lower wheel - in the lower bearing and among the wheels. The gravity force of the upper wheel and the pressing force of the suspension also affect the lower wheel.

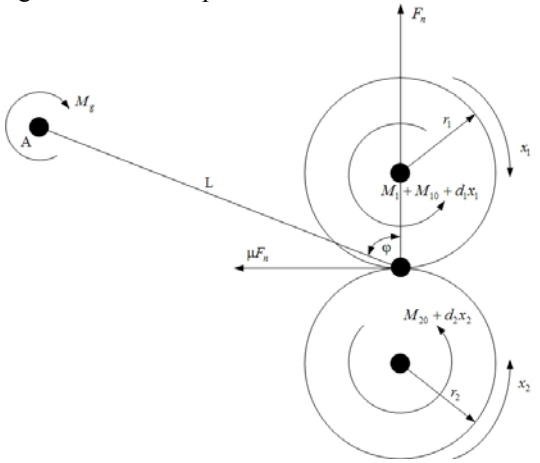

Figure 1. ABS graphical model

Having in mind the previous system description and the graphical representation of ABS depicted in Fig. 1, we derive the ABS dynamical model.

A. Continuous-time ABS model

The upper wheel dynamics can be described as:

$$J_1\dot{x}_1 = F_n r_1 s\mu(\lambda) - d_1 x_1 - s_1 M_{10} - s_1 M_1, \quad (16)$$

where J_1 is a moment of inertia, d_1 is a viscous friction coefficient and M_{10} is a static friction of the upper wheel, $s = \operatorname{sgn}(r_2 x_2 - r_1 x_1)$, $s_1 = \operatorname{sgn}(x_1)$, and x_1 and x_2 are angular velocities of upper and lower wheel, respectively and r_1, r_2 are their radius. F_n represents normal force and $\mu(\lambda)$ is coefficient of proportion called the coefficient of road adhesion, as we mentioned earlier.

The lower wheel dynamics is defined as:

$$J_2\dot{x}_2 = -F_n r_2 s\mu(\lambda) - d_2 x_2 - s_2 M_{20}, \quad (17)$$

where J_2 is a moment of inertia, d_2 is a coefficient of viscous friction, M_{20} is a static friction of the lower wheel, and $s_2 = \operatorname{sgn}(x_2)$. The equations (16) and (17) completely determine the dynamics of the quarter vehicle model given in Fig. 1.

The normal force F_n is supposed to have a constant value in many papers and its perturbations are treated as a non-modelled dynamics. As we do not use such modelling approach, we should derive the normal force F_n from the sum of torques acting at the point A (see Fig. 1) in the following form:

$$F_n = \frac{\left(M_g + s_1 M_1 + s_1 M_{10} + d_1 x_1\right)}{L\left(\sin\varphi - s\mu(\lambda)\cos\varphi\right)}, \quad (18)$$

where M_g represents torque acting on the balance lever (point A in Fig. 1), L is a distance between the contact point of the wheels and point A and φ is the angle between the normal in the contact point and the line L.

The angular velocity of the wheel and the forward velocity of the vehicle match each to other in the normal operating conditions, whereas in the braking and the acceleration phases, they differ one from another. This relative difference of velocities is called a wheel slip λ. The wheel slip is defined in [38] for all operating conditions of the quarter vehicle model.

The coefficient of road adhesion μ is in nonlinear dependence on the wheel slip λ, and one of its possible models is given by:

$$\mu(\lambda) = \frac{w_4\lambda^p}{a+\lambda^p} + w_3\lambda^3 + w_2\lambda^2 + w_1\lambda, \quad (19)$$

where a, p and w_i, $i = \overline{1,4}$, are the real constants given in [38].

By replacing (18) in (16) and (17), we can define ABS model in the following form:

$$\begin{aligned}
\dot{x}_1 &= S(\lambda, x_1, x_2)\left(c_{11}x_1 + c_{12}\right) + c_{13}x_1 + c_{14} + \\
&+ \left(c_{15}S(\lambda, x_1, x_2) + c_{16}\right)s_1(x_1)M_1, \\
\dot{x}_2 &= S(\lambda, x_1, x_2)\left(c_{21}x_1 + c_{22}\right) + c_{23}x_1 + c_{24} + \\
&+ c_{25}S(\lambda, x_1, x_2)s_1(x_1)M_1,
\end{aligned} \quad (20)$$

where $S(\lambda) = \left(s\mu(\lambda)\right)\Big/\left(L\left(\sin\varphi - s\mu(\lambda)\cos\varphi\right)\right)$,

$c_{11} = \left(r_1 d_1\right)/J_1$, $c_{12} = \left(\left(s_1 M_{10} + M_g\right)r_1\right)\Big/J_1$, $c_{13} = -d_1/J_1$,

$c_{14} = -\left(s_1 M_{10}\right)/J_1$, $c_{15} = r_1/J_1$, $c_{16} = -1/J_1$,

$c_{21} = -\left(r_2 d_1\right)/J_2$, $c_{22} = -\left(\left(s_1 M_{10} + M_g\right)r_2\right)\Big/J_2$,

$c_{23} = -d_2/J_2$, $c_{24} = -\left(s_2 M_{20}\right)/J_2$, $c_{25} = -r_2/J_2$.

The braking phase starts after acceleration, when the lower wheel is speed up to 70 km/h. The wheel speed decreases and the force acting on the wheel causes the slippage between the road surface and the tire. The wheel speed is less than vehicle speed, i.e., $r_2 x_2 \geq r_1 x_1$, $x_1 > 0$, $x_2 > 0$, and wheel slip is defined by:

$$\lambda = \frac{r_2 x_2 - r_1 x_1}{r_2 x_2}. \quad (21)$$

If the wheel slip has a zero value, the wheel is not rotating and there is no motion of the vehicle. The wheels will be skidding on the road surface if the slip is equal to one. The consequence is that the vehicle is no steerable anymore.

ABS controller should be designed to regulate the wheel slip at a preset reference value, so that the coefficient of road adhesion has maximum value. Therefore, we should determine ABS model with wheel slip as a controlled variable. By differentiating (21) and by putting (20) in the obtained result, someone gets:

$$\dot{\lambda} = f(\lambda, x_2) + g(\lambda, x_2)M_1, \quad x_2 \neq 0, \quad (22)$$

where

$$\begin{aligned}
f(\lambda, x_2) = &-\left(\left(S(\lambda)c_{11} + c_{13}\right)(1-\lambda) + \frac{r_1}{r_2 x_2}\left(S(\lambda)c_{12} + c_{14}\right)\right) + \\
&+ \frac{(1-\lambda)}{x_2}\left(\left(S(\lambda)c_{21}\frac{r_2}{r_1}(1-\lambda) + c_{23}\right)x_2 + S(\lambda)c_{22} + c_{24}\right),
\end{aligned} \quad (23)$$

$$g(\lambda, x_2) = -\frac{r_1}{r_2 x_2}\left(c_{15}S(\lambda) + c_{16} - \frac{r_2}{r_1}c_{25}S(\lambda)(1-\lambda)\right). \quad (24)$$

The final continuous-time mathematical model of ABS is given by (22). In order to design the closed loop system dynamics with digital SMC, we should obtain the appropriate ABS model in discrete time.

B. Discrete-time ABS model

The simplest way to obtain discrete-time model of (22) is to use the Euler's forward method where the first time-derivative is approximated by $d(\cdot)/dt \sim \left((\cdot)_{k+1} - (\cdot)_k\right)/T$, with T denoting a sampling period. Then, the model (22) can be rewritten as:

$$\lambda_{k+1} = f_k^d + g_k^d M_{1k}, \quad (25)$$

where $f_k^d = \lambda_k + Tf_k(\lambda, x_2)$, $g_k^d = Tg_k(\lambda, x_2)$, and f_k, g_k,

and M_{1k} are sampled values of f, g and M_1 at time-instant k. f_k^d and g_k^d represent smooth nonlinear functions, and it is assumed that the function g_k^d is strictly positive and bounded away from zero. The system must have stable and convergent zero dynamics, as well [39]. Notice that the plant model is linear in relation to the control input M_{1k}.

V. Implementation of Digital SMC Algorithm on ABS

As in the general case (elaborated in Section II), due to parameter uncertainties, we use the nominal model of ABS in design of digital SMC:

$$\hat{\lambda}_{k+1} = \hat{f}_k^d + \hat{g}_k^d M_{1k}, \tag{26}$$

with $\hat{f}_k^d$ and $\hat{g}_k^d$ denoting nominal values of the functions f_k^d and g_k^d, respectively. The modelling error is defined by:

$$\varepsilon_{k+1} = \lambda_{k+1} - \hat{\lambda}_{k+1} = f_k^d - \hat{f}_k^d + \left(g_k^d - \hat{g}_k^d\right) M_{1k}, \tag{27}$$

and it also satisfies (4). Equation (25) can be rewritten now as:

$$\lambda_{k+1} = \varepsilon_{k+1} + \hat{f}_k^d + \hat{g}_k^d M_{1k}. \tag{28}$$

As ABS model is of the first order, the signal error e_k represents the switching function s_k at the same time, i.e.:

$$s_k = e_k = \lambda_k - \lambda_k^{ref}. \tag{29}$$

In order to provide a zero value of the switching function, i.e. the error signal, the proposed control law, given by (9), is modified in the case of ABS and it becomes:

$$M_{1k} = -\frac{1}{\hat{g}_k^d}\left(\hat{f}_k^d - \lambda_{k+1}^{ref} + \frac{\alpha T}{1-z^{-1}}\operatorname{sgn}\left(s_k\right) + \varepsilon_k\right), \tag{30}$$

where $\lambda_{k+1}^{ref} = \lambda_k^{ref} = \text{const.}$, as we consider the control system of regulator-type, and ε_k is an output of one-step delayed modelling error estimator:

$$\varepsilon_k = \lambda_k - \hat{f}_{k-1}^d - \hat{g}_{k-1}^d M_{1k-1}. \tag{31}$$

The switching function dynamics is defined by (11), whereas the control parameter α is selected in accordance with (12).

VI. Experimental Results

The proposed digital SMC algorithm is practically verified on the experimental ABS setup described earlier, which enables users to check their control algorithms in MATLAB and Simulink environment. The experimental results of ABS with the proposed digital SMC are compared with the results obtained by implementation of two other control laws. The first one is taken from [34] and slightly modified as:

$$M_{1k} = -\frac{1}{\hat{g}_k^d}\left(\hat{f}_k^d - \lambda_{k+1}^{ref} - s_k + \beta\operatorname{sgn}\left(s_k\right)\right), \tag{32}$$

to provide switching function dynamics in the form of:

$$s_{k+1} = s_k - \beta\operatorname{sgn}\left(s_k\right) + c_0\varepsilon_{k+1}, \tag{33}$$

whose stability and, consequently, quasi-sliding motion is ensured if:

$$\beta > \max\left|c_0\varepsilon_{k+1}\right|. \tag{34}$$

Thanks to the introduced modifications of control algorithm, the system stability proof can be obtained in similar way as it is given in Theorems 1 and 2. System steady-state accuracy is now determined by the value of $\max\left|c_0\varepsilon_{k+1}\right|$. Therefore, we can expect worse results in comparison to the proposed digital SMC.

The second control law used in experimental validation is a digital SMC algorithm (30) without the one-step modelling error estimator:

$$M_{1k} = -\frac{1}{\hat{g}_k^d}\left(\hat{f}_k^d - \lambda_{k+1}^{ref} + \frac{\alpha T}{1-z^{-1}}\operatorname{sgn}\left(s_k\right)\right), \tag{35}$$

yielding switching function dynamics:

$$s_{k+1} = s_k - \alpha T\operatorname{sgn}\left(s_k\right) + c_0\left(\varepsilon_{k+1} - \varepsilon_k\right). \tag{36}$$

Quasi-sliding mode exists if:

$$\alpha T > \max\left|c_0\left(\varepsilon_{k+1} - \varepsilon_k\right)\right|, \tag{37}$$

and system steady-state accuracy depends on $\max\left|c_0\left(\varepsilon_{k+1} - \varepsilon_k\right)\right|$. The control (35) provides the better accuracy than the control algorithm (32), but the worse one than the control law (30). Theorems 1 and 2 could also be used in the altered version to prove the stability of system with (35) in quasi-sliding mode.

The Figs. 2-5 present the wheel slip responses, obtained by using above mentioned control algorithms. The reference wheel slip is $\lambda_{k+1}^{ref} = 0.2$, except in Fig. 5 where $\lambda_{k+1}^{ref} = 0.3$. The sampling period T is 0.005 s.

Fig. 2 represents the results of wheel slip response with control algorithm (32). The parameter β is equal to 0.1, and, as one can notice, corresponds to αT in remaining control algorithms. This produces notable oscillations around the reference wheel slip and wider quasi-sliding manifold.

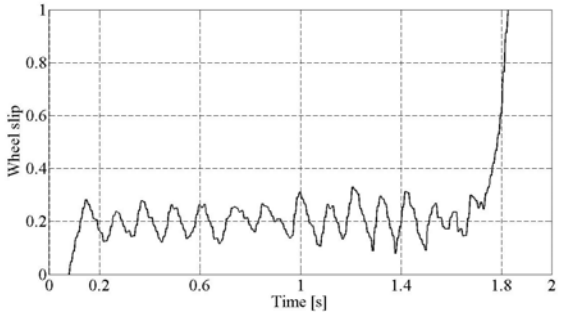

Figure 2. Wheel slip response with control (32)

The implementation of (35) in control of ABS gives response shown in Fig. 3. Besides the effects of chattering reduction, enabled by filtering of relay control term through digital integrator, this digital SMC provides quasi-sliding motion with smaller control signal efforts. Namely, the parameter α is chosen to be 1. Unfortunately, although system steady-state accuracy should be theoretically within $\sim \alpha T = 5\times10^{-3}$ boundaries, due to noise and un-modelled dynamics it is in a wider range. However, the error signal is smaller than in the previous case when control (32) is applied on ABS.

The best wheel slip response is obtained by using the novel digital SMC proposed herein. The results are presented in Fig. 4 and Fig. 5 for $\lambda_{k+1}^{ref} = 0.2$ and $\lambda_{k+1}^{ref} = 0.3$,

respectively. The parameter α is taken to be 10 times smaller than in the previous control law, i.e., $\alpha = 0.1$, and consequently $\alpha T = 5\times10^{-4}$.

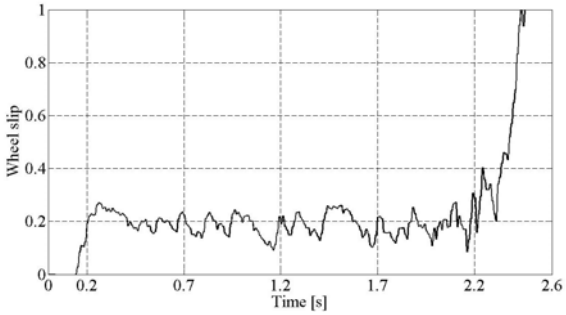

Figure 3. Wheel slip response with control (35)

The chattering is also alleviated thanks to the filtering of the relay control term by the digital integrator. The introduction of one-step delayed modelling error estimator signal in control law has the same effect as an implementation of one additional integrator in control [32]. This causes better system steady-state accuracy than with the implementation of two previously discussed algorithms.

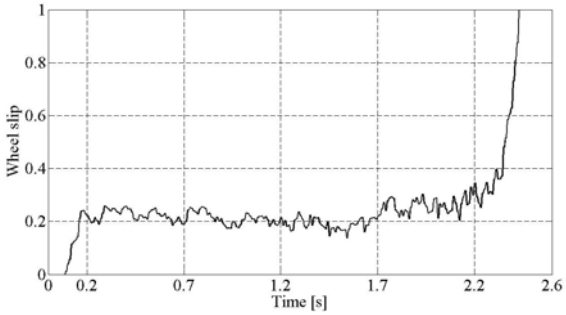

Figure 4. Wheel slip response with the proposed control (30) for $\lambda_{k+1}^{ref} = 0.2$

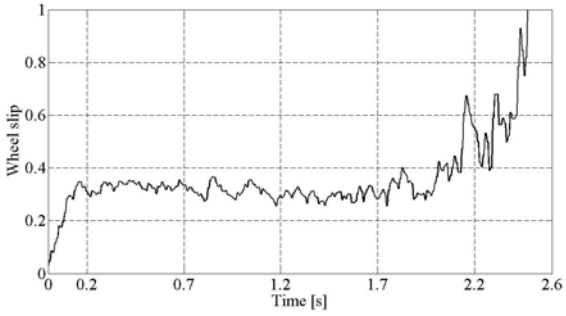

Figure 5. Wheel slip response with the proposed control (30) for $\lambda_{k+1}^{ref} = 0.3$

VII. Conclusion

This paper deals with a new approach in the design of digital sliding mode control for anti-lock braking system (ABS). The proposed digital sliding mode control (SMC) is based on the input/output discrete-time non-linear model of the plant. It is characterized by alleviated chattering phenomenon, since digital integrator filters the relay control component. The introduction of one-step delayed modelling error estimator additionally enlarges the system accuracy. The continuous- and discrete-time mathematical models of ABS are derived first, and, then, the proposed digital SMC is accommodated to cope with the obtained discrete-time ABS model. Finally, the control algorithm is compared with two other digital SMC laws through real experiment. Experimental results confirmed good performances of the given control and its superiority over the existing digital SMC solutions.

Appendix A

First, we will prove that s_k enters the domain $S(T)$ in finite time, and, then, show that s_k remains in that area. Suppose that (s_k), defined by (11), is a positive sequence. The proof is similar when (s_k) is negative sequence. Then:

$$\begin{aligned} &s_{k+1} - s_k = -\alpha T + c_o\left(\varepsilon_{k+1} - 2\varepsilon_k + \varepsilon_{k-1}\right) < \\ &< -\alpha T + \Delta\mathrm{E} < 0\,, \end{aligned} \tag{A1}$$

is valid if (12) is satisfied, i.e. $s_{k+1} < s_k$ and:

$$0 < \frac{s_{k+1}}{s_k} = q_k < 1\,. \tag{A2}$$

There exists a positive number δ satisfying the following inequality:

$$\left|s_{k+1} - s_k\right| = \left|s_0\left(\prod_{i=0}^{k-1} q_i\right)(q_k - 1)\right| < \delta\,, \tag{A3}$$

as $\prod_{i=0}^{k-1} q_i < 1$ and $q_k < 1$. Therefore, based on Cauchy's theorem of sequence convergence, we conclude that sequence (s_k) is convergent. The convergence domain of sequence (s_k) is:

$$\overline{S}(T) = \left\{s_k : \left|s_k\right| > \alpha T + \Delta\mathrm{E}\right\}. \tag{A4}$$

Namely $0 < s_{k+1}/s_k < 1$ implies $0 < \left(\alpha T \operatorname{sgn}(s_k) - c_o\left(\varepsilon_{k+1} - 2\varepsilon_k + \varepsilon_{k-1}\right)\right)/s_k < 1$, directly giving (A4) for both positive and negative sequence (s_k).

Let us show that system trajectory enters domain $S(T)$ in finite time. Sequence (s_k) converges into the domain $\overline{S}(T)$, so it is limited, i.e.: $\lim_{k\to\infty} s_k = s_\infty$. Assume that $s_0 > \alpha T + \Delta\mathrm{E}$ is satisfied. According to (11):

$$s_k = s_0 - \sum_{i=0}^{k-1}\left(\alpha T - c_o\left(\varepsilon_{i+1} - 2\varepsilon_i + \varepsilon_{i-1}\right)\right). \tag{A5}$$

Suppose that s_k never enters the domain $S(T)$. When $k \to \infty$, we can obtain straightforward from (A5) the following inequality:

$$\sum_{i=0}^{\infty}\left(\alpha T - c_o\left(\varepsilon_{i+1} - 2\varepsilon_i + \varepsilon_{i-1}\right)\right) < s_0 - \alpha T - \Delta\mathrm{E}\,, \tag{A6}$$

implying that the series $\sum_{i=0}^{\infty}\left(\alpha T - c_o\left(\varepsilon_{i+1} - 2\varepsilon_i + \varepsilon_{i-1}\right)\right)$ is convergent, and its general element $\alpha T - c_o\left(\varepsilon_{i+1} - 2\varepsilon_i + \varepsilon_{i-1}\right)$ converges to zero as $i \to \infty$, i.e.:

$$\alpha T = \lim_{i\to\infty}\left(c_o\left(\varepsilon_{i+1} - 2\varepsilon_i + \varepsilon_{i-1}\right)\right), \tag{A7}$$

which is opposite to the condition (12) of Theorem 1. Therefore, the assumption that s_k never enters the domain $S(T)$ is false. The proof is similar for $s_0 < -\alpha T - \Delta\mathrm{E}$. Moreover, s_k enters the domain $S(T)$ at $k = K_0$,

determined by

$$K_0 = \text{int}\left(\left(|s_0| - \alpha T - \Delta\text{E}\right)/\left(\alpha T - \Delta\text{E}\right)\right) + 1. \quad \text{(A8)}$$

We will now show that for every $k > K_0$, s_k remains in the domain $S(T)$.

Let $s_{K_0} \in S^+(T) = \{s_k : 0 < s_k < \alpha T + \Delta\text{E}\}$. Then, according to (11), we have:

$$\begin{aligned} &-\alpha T - \Delta\text{E} \underset{(12)}{<} s_{K_0} - \alpha T + c_o\left(\varepsilon_{K_0+1} - 2\varepsilon_{K_0} + \varepsilon_{K_0-1}\right) = \\ &= s_{K_0+1} \underset{(12)}{<} 2\Delta\text{E} \underset{(12)}{<} \alpha T + \Delta\text{E}, \end{aligned} \quad \text{(A9)}$$

and s_k do not leave domain $S(T)$. This is also true when $s_{K_0} \in S^-(T) = \{s_k : -\alpha T - \Delta\text{E} < s_k < 0\}$ since:

$$\begin{aligned} &-\alpha T - \Delta\text{E} \underset{(12)}{<} -2\Delta\text{E} \underset{(12)}{<} s_{K_0+1} = \\ &= s_{K_0} + \alpha T + c_o\left(\varepsilon_{K_0+1} - 2\varepsilon_{K_0} + \varepsilon_{K_0-1}\right) \underset{(12)}{<} \alpha T + \Delta\text{E}. \end{aligned} \quad \text{(A10)}$$

The case when $s_{K_0+1} < 0$ and $s_{K_0+1} \notin S(T)$ for $s_0, s_{K_0} > \alpha T + \Delta\text{E}$ is not possible as:

$$\begin{aligned} &s_{K_0+1} = s_{K_0} - \alpha T + c_o\left(\varepsilon_{K_0+1} - 2\varepsilon_{K_0} + \varepsilon_{K_0-1}\right) > \\ &> \Delta\text{E} + c_o\left(\varepsilon_{K_0+1} - 2\varepsilon_{K_0} + \varepsilon_{K_0-1}\right) > 0. \end{aligned} \quad \text{(A11)}$$

The case when $s_{K_0+1} > 0$ and $s_{K_0+1} \notin S(T)$ for $s_0, s_{K_0} < -\alpha T - \Delta\text{E}$ cannot happen as well, since:

$$\begin{aligned} &s_{K_0+1} = s_{K_0} + \alpha T + c_o\left(\varepsilon_{K_0+1} - 2\varepsilon_{K_0} + \varepsilon_{K_0-1}\right) < \\ &< -\Delta\text{E} + c_o\left(\varepsilon_{K_0+1} - 2\varepsilon_{K_0} + \varepsilon_{K_0-1}\right) < 0. \end{aligned} \quad \text{(A12)}$$

Therefore, we have proven that $s_{K_0+1} \in S(T)$ and, by using the mathematical induction method, we can generalize it to:

$$s_{K_0+m} \in S(T), \quad \text{(A13)}$$

for every m, representing randomly selected positive integer number. Having demonstrated that (A13) is satisfied if (12) is valid, the proof ends.

REFERENCES

[1] A. Zanten, R. Erhardt, A. Lutz, "Measurement and simulation of transients in long-tudinal and lateral tire forces," in *Proc. of the International Congress & Exposition*, Detroit, USA, February 1990, vol. 99, no. 6, pp. 300–318.

[2] M. Tanelli, L. Piroddi, S. M. Savaresi, "Real-time identification of tire-road friction conditions," IET Control Theory and Applications, vol. 3, no. 7, pp. 891–906, 2009. [Online]. Available: http://dx.doi.org/10.1049/iet-cta.2008.0287

[3] A. Aly, E.-S. Zeidan, A. Hamed, F. Salem, "An antilock-braking systems (ABS) control: A technical review," Intelligent Control and Automation, vol. 2, pp. 186–195, 2011. [Online]. Available: http://dx.doi.org/10.4236/ica.2011.23023

[4] R.-E. Precup, S. Preitl, B. M. Rădac, E. M. Petriu, C. A. Dragoş, J. K. Tar, "Experiment-based teaching in advanced control engineering," IEEE Transactions on Education, vol. 54, no. 3, pp. 345–355, 2011. [Online]. Available: http://dx.doi.org/10.1109/TE.2010.2058575

[5] A. B. Sharkawy, "Genetic fuzzy self-tuning PID controllers for antilock braking systems," Engineering Applications of Artificial Intelligence, vol. 23, no. 7, pp. 1041–1052, 2010. [Online]. Available: http://dx.doi.org/10.1016/j.engappai.2010.06.011

[6] R.-E. Precup, S. Preitl, M. Bălaş, V. Bălaş, "Fuzzy controllers for tire slip control in anti-lock braking systems," in *Proc. of the IEEE International Conference on Fuzzy Systems*, Budapest, Hungary, July 2004, vol. 3, pp. 1317–1322. [Online]. Available: http://dx.doi.org/10.1109/FUZZY.2004.1375359

[7] R.-E. Precup, S. V. Spătaru, M.-B. Rădac, E. M. Petriu, S. Preitl, C.-A. Dragoş, "Model-based fuzzy control solutions for a laboratory antilock braking system," in *Proc. of 3rd International Conference on Human System Interaction, HSI 2010*, Rzeszow, Poland, May 2010, pp. 133-138. [Online]. Available: http://dx.doi.org/10.1109/HSI.2010.5514577

[8] J.-S. Lin, W.-E. Ting, "Nonlinear control design of anti-lock braking systems with assistance of active suspension," IET Control Theory and Applications, vol. 1, no. 1, pp. 343–348, 2007. [Online]. Available: http://dx.doi.org/10.1049/iet-cta:20050218

[9] J. Y. Hung, W. Gao, J. C. Hung, "Variable structure control: A survey," IEEE Transactions on Industrial Electronics, vol. 40. no. 1, pp. 2–22, 1993. [Online]. Available: http://dx.doi.org/10.1109/41.184817

[10] V. I. Utkin, "Sliding mode control design principles and application to electric drives," IEEE Transactions on Industrial Electronics, vol. 40, no. 1, pp. 23–36, 1993. [Online]. Available: http://dx.doi.org/10.1109/41.184818

[11] A. Tahour, H. Abid, A. G. Aissaoui, "Speed control of switched reluctance motor using fuzzy sliding mode," Advances in Electrical and Computer Engineering, vol. 8, no. 1, pp. 21–25, 2008. [Online]. Available: http://dx.doi.org/10.4316/AECE.2008.01004

[12] M. Sarailoo, Z. Rahmani, B. Rezaie, "Fuzzy sliding mode control for hyper chaotic Chen system," Advances in Electrical and Computer Engineering, vol. 12, no. 1, pp. 85–90, 2012. [Online]. Available: http://dx.doi.org/10.4316/AECE.2012.01014

[13] E. Kayacan, Y. Oniz, O. Kaynak, "A grey system modeling approach for sliding-mode control of antilock braking systems," IEEE Transactions on Industrial Electronics, vol. 56, no. 8, pp. 3244–3252, 2009. [Online]. Available: http://dx.doi.org/10.1109/TIE.2009.2023098

[14] K. Chun, M. Sunwoo, "Wheel slip control with moving sliding surface for traction control system," International Journal of Automotive Technology, vol. 5, no. 2, pp. 123–133, 2004. [Online]. Available: http://ref.daum.net/item/528434

[15] A. Harifi, A. Aghagolzadeh, G. Alizadeh, M. Sadeghi, "Designing a sliding mode controller for slip control of antilock brake systems," Transportation Research Part C: Emerging Technologies, vol. 16, no. 6, pp. 731–741, 2008. [Online]. Available: http://dx.doi.org/10.1016/j.trc.2008.02.003

[16] E. J. Park, D. Stoikov, L. Falcao, A. Suleman, "A performance evaluation of an automotive magnetorheological brake design with a sliding mode controller," Mechatronics, vol. 16, no. 7, pp. 405–416, 2006. [Online]. Available: http://dx.doi.org/10.1016/j.mechatronics.2006.03.004

[17] N. Hamzah, M. Y. Sam, A. A. Basari, "Enhancement of driving safety feature via sliding mode control approach," in *Proc. of the 4th International Conference on Computational Intelligence, Robotics and Autonomous Systems*, Palmerston North, New Zealand, 2007, pp. 116–120. [Online]. Available: http://eprints.utm.my/13956/

[18] C. Unsal, P. Kachroo, "Sliding mode measurement feedback control for antilock braking systems," IEEE Transactions on Control Systems Technology, vol. 7, no. 2, pp. 271–281, 1999. [Online]. Available: http://dx.doi.org/10.1109/87.748153

[19] A. El Hadri, J. C. Cadiou, N. K. M'sirdi, "Adaptive sliding mode control of vehicle traction," in *Proc. of the 15th Triennial World Congress*, Barcelona, Spain, June 2002. [Online]. Available: http://dx.doi.org/10.3182/20020721-6-ES-1901.01533

[20] Y. Jing, Y. Mao, G. M. Dimirovski, Y. Zheng, S. Zhang, "Adaptive global sliding mode control strategy for the vehicle antilock braking systems," in *Proc. of the 28th American Control Conference*, St. Louis, Missouri, 2009, pp. 769–773. [Online]. Available: http://dx.doi.org/10.1109/ACC.2009.5160357

[21] M. Wu, M. Shih, "Using the sliding-mode PWM method in an anti-lock braking system," Asian Journal of Control, vol. 3, no. 3, pp. 255–261, 2001. [Online]. Available: http://dx.doi.org/10.1111/j.1934-6093.2001.tb00065.x

[22] M. Wu, M. Shih, "Simulated and experimental study of hydraulic anti-lock braking system using sliding-mode PWM control," Mechatronics, vol. 13, no. 4, pp. 331–351, 2003. [Online]. Available: http://dx.doi.org/10.1016/S0957-4158(01)00049-6

[23] H. Mirzaeinejad, M. Mirzaei, "A novel method for non-linear control of wheel slip in anti-lock braking systems," Control Engineering Practice, vol. 18, no. 8, pp. 918–926, 2010. [Online]. Available: http://dx.doi.org/10.1016/j.conengprac.2010.03.015

[24] S. Zheng, H. Tang, Z. Han, Y. Zhang, "Controller design for vehicle stability enhancement," Control Engineering Practice, vol. 14, no. 12, pp. 1413–1421, 2006. [Online]. Available: http://dx.doi.org/10.1016/j.conengprac.2005.10.005

[25] D. Mitić, D. Antić, S. Perić, M. Milojković, S. Nikolić, "Fuzzy sliding mode control for anti-lock braking systems," in *Proc. of the 7th International Symposium on Applied Computational Intelligence and Informatics, SACI 2012*, Timisoara, Romania, May 2012, pp. 217–222. [Online]. Available: http://dx.doi.org/10.1109/SACI.2012.6250005

[26] W. Gao, J. C. Hung, "Variable structure control of nonlinear systems: A new approach," IEEE Transactions on Industrial Electronics, vol. 40, no. 1, pp. 45–55, 1993. [Online]. Available: dx.doi.org/10.1109/41.184820

[27] D. Antić, V. Nikolić, D. Mitić, M. Milojković, S. Perić, "Sliding mode control of anti-lock braking system: An overview," FACTA UNIVERSITATIS Series: Automatic Control and Robotics, vol. 9, no. 1, pp. 41–58, 2010, [Online]. Available: http://facta.junis.ni.ac.rs/acar

[28] Č. Milosavljević, "General conditions for the existence of a quasi-sliding mode on the switching hyperplane in discrete variable structure systems," Automatic Remote Control, vol. 46, pp. 307–314, 1985.

[29] Č. Milosavljević, "Discrete-time VSS", in Variable Structure Systems: from Principles to Implementation, A. Šabanović, L. Fridman, S. Spurgeon, (Eds.), IEE Control Engineering, London, Series 66, pp. 99–129, 2004.

[30] M. L. Corradini, G. Orlando, "Discrete variable structure control for nonlinear systems," in *Proc. of 3rd European Control Conference*, Rome, Italy, 1995, pp.1465–1470.

[31] K. Furuta, "VSS type self-tuning control," IEEE Transaction on Industrial Electronics, vol. 40, no. 1, pp. 37–44, 1993. [Online]. Available: http://dx.doi.org/10.1109/41.184819

[32] D. Mitić, Digital variable structure systems based on input-output model. PhD thesis, University of Niš, Faculty of Electronic Engineering, 2006, (in Serbian).

[33] D. Mitić, Č. Milosavljević, "Sliding mode based minimum variance and generalized minimum variance controls with $O(T^2)$ and $O(T^3)$ accuracy," Electrical Engineering, vol. 86, pp. 229–237, 2004. [Online]. Available: http://dx.doi.org/10.1007/s00202-003-0198-y

[34] D. Munoz, D. Sbarbaro, "An adaptive sliding-mode controller for discrete nonlinear systems," IEEE Transactions on Industrial Electronics, vol. 47, no. 3, pp. 574–581, 2000. [Online]. Available: http://dx.doi.org/10.1109/41.847898

[35] H.-S. Tan, M. Tomizuka, "Discrete-time controller design for robust vehicle traction," IEEE Control Systems Magazine, vol. 10, no. 3, pp. 107–113, 1990. [Online]. Available: http://dx.doi.org/10.1109/37.55132

[36] D. Mitić, Č. Milosavljević, B. Veselić, "One approach to I/O based design of digital sliding mode control for nonlinear plants," Electronics, vol. 8, no. 2, pp. 64–67, 2004. [Online]. Available: http://www.electronics.etfbl.net

[37] D. Mitić, Č. Milosavljević, B. Peruničić-Draženović, B. Veselić, "Digital sliding mode control design based on I/O model of nonlinear plants", in *Proc. of IEEE 9th International Workshop on Variable Structure Systems*, Alghero, Sardinia, Italy, June 2006, pp. 57–62. [Online]. Available: http://www.diee.unica.it/vss06

[38] Inteco, "The laboratory anti-lock braking system controlled from PC-User's manual", 2008. [Online]. Available: www.inteco.com.pl

[39] F. C. Chen, H. Khalil, "Adaptive control of a class of nonlinear discrete-time systems using neural networks," IEEE Transactions of Automatic Control, vol. 40, pp.791–797, 1995. [Online]. Available: http://dx.doi.org/10.1109/9.384214